EURASIAN PHYSICAL TECHNICAL JOURNAL

2026, Volume 23, No. 1(55)

https://doi.org/10.31489/2026N1/48-59

Received: 18/11/2025 Revised: 29/01/2026 Accepted: 19/03/2026 Published online: 30/03/2026

Research Article

UDC 53.662

OPTIMIZATION OF THERMAL PROCESSES IN SOLAR BIOGAS PLANT

Sharipov M.Z.[1*], Majitov J.A.[2], Imomov Sh.J.[3], Kovalev I.V.[4], Narzullayev M.N.[5], Negmatillayev B.[2], Ziyoyev D.A[2]

[1] Bukhara State University, Bukhara, Uzbekistan
[2] Bukhara State Technical University, Bukhara, Uzbekistan
[3] Tashkent Institute of Irrigation and Agricultural Mechanization Engineers "National Research University", Tashkent, Uzbekistan
[4] Siberian Federal University, Krasnoyarsk, Russia
[5] Bukhara State Pedagogical Institute, Bukhara, Uzbekistan

*Corresponding author: m.z.sharipov@rambler.ru

Abstract. *This article presents the results of research devoted to improving the thermal regime of a small-scale biogas plant operating under the conditions of Uzbekistan and utilizing solar energy. The study optimized the constructive and energetic parameters of a cylindrical solar-heated biogas plant. The main part of the plant is a bioreactor equipped with a solar heating system, designed for anaerobic fermentation of organic materials to produce biogas and organic fertilizer (humus). During the research, the amount of solar radiation, daily variations of ambient and bioreactor temperatures, and the dynamics of biogas production were analyzed. The results showed a stable increase in biogas production, which demonstrates the efficiency of using solar energy and highlights the importance of maintaining the optimal thermal regime of the bioreactor. Changes in the composition of biogas under mesophilic and psychrophilic regimes were also studied. The final conclusion emphasizes that temperature plays a key role in ensuring the stability of the fermentation process in small-capacity biogas plants, and that mathematical modeling of thermal processes is essential.*

Keywords: *solar energy, mesophilic, psychrophilic, biogas, fertilizer, reactor, absorber, heat accumulator, thermal insulation, thermostat, plastic pipe, spiral, collector.*

1. Introduction

Solar-assisted anaerobic digestion systems are thermo-physical systems whose efficiency is determined by the stability of the reactor temperature under mesophilic conditions (36–37 °C) [1-6]. For small-capacity cylindrical reactors, maintaining this temperature requires compensation of conductive and convective heat losses through the reactor walls. The paper by Perrigault et al. [7] presents a time-dependent thermal model of a digester using climatic input parameters (solar radiation, wind speed, ambient temperature) and reactor geometry. It was shown that environmental conditions significantly influence internal temperature distribution and heat losses. However, the study was focused on transient simulation and did not address structural optimization of reactor walls or insulation thickness as an energy-efficiency problem. A related parametric analysis of thermal-technical and geometric characteristics of a small-scale biogas plant was presented in [8], where substitution of structural parameters was investigated. It was shown that reactor dimensions significantly affect thermal performance. However, the quantitative role of multilayer wall resistance and insulation

thickness under real solar loading conditions was not fully evaluated. Numerical modeling of heat exchange processes in individual bioenergy installations was also reported in [9], confirming the sensitivity of temperature stabilization to external climatic conditions. Nevertheless, the coupled problem of optimizing collector performance and cylindrical wall heat resistance remains insufficiently resolved.

The utility model patent "Solar biogas plant" [10] proposes a constructive solution integrating a solar collector and phase-change thermal storage. Experimental solar thermal systems of combined type are described in [11], demonstrating the practical feasibility of solar heat supply for decentralized installations. However, neither [10] nor [11] provides a thermo-physical justification of insulation parameters, equivalent thermal resistance of the cylindrical wall, or a quantitative analysis of heat-loss minimization. As a result, the energy-saving effect of the proposed structures remains insufficiently quantified. The difficulty of optimizing energy-saving structures in small-scale systems is associated with the coupled influence of geometry, surface-to-volume ratio, convective boundary conditions, and multilayer conductive resistance. Excessive insulation increases construction cost, while insufficient insulation leads to thermal instability and additional collector load. In addition, maintaining stable microbial activity under mesophilic conditions requires controlled thermal regimes, as noted in studies of bioenergy system stability [12]. A systematic heat-transfer analysis of the reactor as a multilayer cylindrical body is therefore required.

In this work, the reactor is considered as a multilayer cylindrical heat-transfer system with solar heat input and external convective boundary conditions. The scientific novelty of the study consists in: quantitative evaluation of the equivalent thermal resistance of the reactor wall as a function of insulation thickness; determination of rational insulation parameters ensuring stable mesophilic temperature under real climatic conditions; experimental validation of the calculated heat-loss characteristics for a small-capacity solar collector biogas plant; and assessment of the interaction between solar heat supply and phase-change thermal accumulation in maintaining thermal stability. The relevance of the proposed approach is consistent with modern developments in renewable agrotechnological systems [13], where analytical optimization of thermal regimes is considered a key factor of decentralized energy efficiency.

Thus, the study aims to justify energy-saving structural parameters of a small-capacity solar biogas reactor based on a combined analytical and experimental heat-transfer analysis.

2. Main Part

2.1. Object of Research

The object of research is a small-capacity solar-assisted biogas plant operating under mesophilic conditions (36–37 °C). From a thermo-physical viewpoint, the system is considered as a multilayer cylindrical reactor subjected to solar heat input and external convective heat losses.

The structural configuration of the experimental device is presented in Fig. 1. The central element of the system is a cylindrical fermentation reactor (1) containing the biomass (9). The reactor is placed inside an external cylindrical vessel forming a water jacket (2, 4). A spiral heat exchanger (3) is installed in the jacket and connected to flat-plate solar collectors (5). Phase-change thermal storage material (19) is arranged around the heat exchanger to accumulate excess solar energy during peak radiation periods. The system also includes external thermal insulation (18), a mixing device (10), gas outlet and purification elements (11-14), biomass loading and discharge units (7, 8, 15), and temperature control components (16, 17).

This configuration allows the reactor to be analyzed as a multilayer cylindrical heat-transfer system consisting of biomass, metallic wall, water jacket, insulation layer, and external convective boundary. The key performance parameter of the system is the ability to maintain a stable internal temperature within the mesophilic range under real climatic conditions.

Prepared biomass intended for fermentation of organic waste is introduced into the reactor through a hatch installed on its side, ensuring that the volume of biomass inside the reactor equals two-thirds of the reactor's total capacity. To reduce heat loss to the external environment, the outer cylindrical vessel is completely covered with thermal insulation [5-8]. To ensure that the fermentation process inside the reactor proceeds uniformly and that biogas is released at a steady rate, a finned mixing device is installed in the center of the reactor, designed for manual operation. For this device, an optimal mixing frequency of 4–5 times per day has been determined, which prevents the formation of a dense layer on the biomass surface that could hinder gas release. The operating principle of the biogas plant is as follows: in the morning, when the sun rises, solar radiation falls on the transparent surface of the solar collectors, passes through it, and is absorbed by a flat metal plate acting as the absorber.

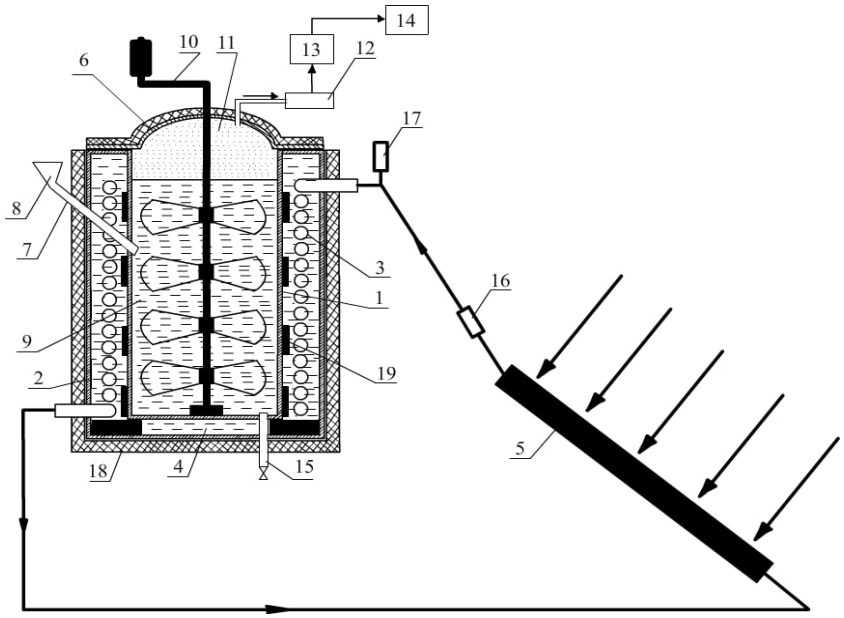

Fig. 1. Schematic diagram of a solar biogas plant. (FAP 2440 19.03.2024): 1 - reactor of biogas device; 2 - water reservoir; 3 - helical heat exchanger made of plastic tube; 4 - water in Reservoir jacket; 5-solar water heater collectors; 6 - reservoir and reactor top seal; 7 and 8 - reactor ready biomass injector Hatch and its throat; 9-biomass in reactor; 10 - mixer device; 11 - formed biogas; 12 - throttle; 13 - gas filter 14 - gas kraynik; 15 - humus release lug; 16 - thermoregulator; 17 - expansion tank; 18 - external thermal insulation; 19 - phase variable heat-collecting material

The absorbed radiation is converted into heat, which warms the water-filled metal fins attached to the plate, thereby heating the water inside the collectors. The heated water in the collectors circulates convectively and passes through a spiral-shaped heat exchanger installed in the water jacket of the external vessel containing the reactor. In doing so, it transfers its thermal potential to the water in the jacket and to the phase-change heat storage materials placed there. After releasing its heat, the water flows back through the lower pipe of the spiral heat exchanger to the solar collectors. The repetition of this process throughout the day ensures uniform heating of the water surrounding the reactor, the heat accumulator, and ultimately the biomass inside the reactor [14].

As phase-change heat accumulators around the spiral heat exchanger, materials are selected whose melting temperatures correspond to the optimal isothermal mesophilic regime. Thus, part of the solar energy received during the day is stored in the phase-change heat accumulator. In the evening or when solar radiation decreases, this stored heat maintains the optimal isothermal process inside the reactor. One of the most important aspects of the ongoing research on this device is the study of the constructive and thermal-energetic characteristics of the solar water-heating collectors and the spiral-shaped heat exchanger connected to them.

2.2. Materials and Methods

The experimental prototype has a total reactor volume of 1.7407 m^3. The working biomass occupies 70% of the total volume (1219 kg at initial loading). Thermophysical parameters used in calculations include: biomass density: 1030 kg/m^3; specific heat capacity: 3.2-3.5 $kJ/(kg\cdot{}^0C)$; operating temperature range: 36–37 ^0C; annual global solar radiation (Bukhara region): 1766 kWh/m^2; solar collector area: 0.745 m^2; collector efficiency: 42.6%.

Solar radiation was measured using a calibrated pyranometer (measurement error ±0.01 W/m^2). Ambient temperature and wind speed were recorded to determine external convective heat-transfer coefficients. Temperature measurements inside the collector loop and reactor were performed using thermocouples connected to a data acquisition system.

The investigation combines analytical modeling and experimental validation of the solar collector–bioreactor thermal system. The methodological framework is based on solving an energy balance problem for a flat-plate solar collector coupled with a multilayer cylindrical bioreactor. The investigation combines analytical modeling and experimental validation.

Analytical Modeling of the Solar Collector

The useful heat gain of the flat-plate solar collector is determined from the steady-state energy balance between absorbed solar radiation and thermal losses to the environment:

$$Q_u = \tau\alpha I_T A_c - U_L A_c\left(T_{pm} - T_a\right) \quad (1)$$

or in compact form:

$$Q_u = A_c\left[\tau\alpha I_T - U_L\left(T_{pm} - T_a\right)\right] \quad (2)$$

where: Q_u - useful heat gain (W); A_c - collector area (m^2); τ - glass cover transmittance; α - absorber absorptance; I_T - incident solar radiation (W/m^2); U_L - overall heat loss coefficient (W/(m^2 ^{0}C)); T_p - mean absorber plate temperature (^{0}C); T_a - ambient temperature (^{0}C).

The instantaneous thermal efficiency of the collector is defined as:

$$\eta_c = \frac{Q_u}{A_c I_T} \quad (3)$$

Substituting Eq. (2) into Eq. (3):

$$\eta_c = \tau\alpha - \frac{U_L(T_{pm} - T_a)}{I_T} \quad (4)$$

The useful heat transferred to the working fluid is also determined experimentally from:

$$Q_u = \dot{m} C_{pf}\left(T_{fo} - T_{fi}\right) \quad (5)$$

where $\dot{m}$ is the mass flow rate of the fluid (kg/s), C_{pf} is its specific heat capacity (J/(kg·^{0}C)), T_{fo} and T_{fi} are outlet and inlet fluid temperatures (^{0}C).

For the stagnation condition ($\dot{m}$=0), the useful heat gain becomes zero:

$$0 = \tau\alpha I_T A_c - U_L A_c (T_s - T_a) \quad (6)$$

which yields the stagnation temperature:

$$T_{st} = T_a + \frac{\tau\alpha I_T}{U_L} \quad (7)$$

These relations provide the basis for determining collector performance parameters under varying climatic conditions.

Modeling of Heat Losses from the Bioreactor

Heat losses from the bioreactor are evaluated by modeling the reactor wall as a multilayer cylindrical system. Radial heat transfer through the wall and insulation layers is described using the equivalent thermal resistance approach. For steady-state radial conduction, the heat flow rate is:

$$Q = \frac{2\pi L\left(T_{pm} - T_a\right)}{\sum_j \frac{\left(r_{j+1}/r_j\right)}{\lambda_j} + \frac{1}{h_{ext} r_{ext}}}$$

where: L - reactor height (m); T_i - internal biomass temperature (^{0}C); r_j - inner radius of layer j; λ_j - thermal conductivity of layer j (W/(m·^{0}C)); h_{ext} - external convective heat transfer coefficient (W/(m^2·^{0}C)); r_{ext} - external radius of the insulated reactor (m).

This formulation allows determination of: the dependence of total heat loss on insulation thickness, the reduction in overall heat transfer coefficient U_L, the influence of external convective conditions (wind speed), and the stabilization effect on biomass temperature.

Assumptions and Applicability of the Thermal Model

The proposed thermal model is based on the following assumptions:

1. Heat transfer is considered quasi-steady during the analyzed time intervals; transient thermal inertia effects are neglected.
2. Radial one-dimensional heat transfer is assumed for the multilayer cylindrical reactor wall; axial gradients are neglected.
3. Thermophysical properties of materials are taken as constant within the mesophilic temperature range (33–40 ^{0}C).
4. Solar radiation is assumed uniformly distributed over the collector surface.

5. The biomass temperature inside the reactor is treated as spatially uniform due to mixing.

The model is applicable under moderate climatic conditions (solar radiation up to 800 W/m^2 and wind speeds up to 5 m/s). For strongly transient regimes or extreme environmental conditions, a time-dependent distributed model would be required.

Experimental measurements included: solar radiation intensity; ambient temperature and wind speed; inlet and outlet temperatures of the heat-transfer fluid; biomass temperature inside the reactor; daily biogas production and methane content. Experimental temperature profiles were compared with analytical predictions to validate the heat-transfer model and to determine rational insulation parameters ensuring thermal stability.

To ensure reliability and reproducibility, experimental measurements were carried out in accordance with internationally recognized standards and recommendations for thermal and biogas systems.

The composition of biogas (CH_4, CO_2 and trace gases) was determined using gas chromatography in accordance with ISO 6976:2016 (Natural gas - Calculation of calorific values, density and Wobbe index) and methodological recommendations for biogas analysis described in VDI 4630 (2016). Methane concentration was calculated as the volumetric fraction (%) based on chromatographic peak area normalization. Calibration of the analyzer was performed using certified reference gas mixtures. Measurement uncertainty of methane content did not exceed ±1.5%.

Temperature measurements were performed using calibrated thermocouples (type K) installed at the inlet and outlet of the collector circuit. The measurement procedure followed the requirements of ISO 9488:1999 (Solar energy - Vocabulary) and recommendations for performance testing of solar collectors according to ISO 9806:2017 (Solar energy - Solar thermal collectors - Test methods). Temperature data were recorded with a time resolution of 5 minutes. The expanded measurement uncertainty of temperature did not exceed ±0.5 ^{0}C.

Global solar radiation was measured using a calibrated pyranometer installed on a horizontal surface without shading, in accordance with ISO 9060:2018 (Solar energy - Specification and classification of instruments for measuring hemispherical solar radiation) and WMO Guide to Meteorological Instruments and Methods of Observation (WMO-No. 8). Data were logged continuously and averaged over 10-minute intervals. The instrumental error of radiation measurements was ±0.01 W/m^2.

Processing of experimental data was performed using standard methods of statistical analysis: arithmetic mean values were calculated for daily temperature and radiation profiles; standard deviation was used to estimate dispersion; relative measurement error was determined using propagation of uncertainty; correlation analysis was applied to evaluate the relationship between biomass temperature and methane production rate. All reported results correspond to averaged values with indicated measurement uncertainties.

3. Results and Discussion

3.1. Analysis of Insulation Thickness and Heat-Loss Reduction

In the experiments, to measure the solar radiation falling on the experimental device, the pyranometer was installed on a horizontal surface without any obstacles. The output data from the pyranometer were recorded in a data log, and these records were then used to calculate the total amount of solar radiation received over a certain period of time. In the research site in Bukhara city during the summer months, the maximum average value of global solar radiation is approximately 800 W/m^2, which occurs at midday, while the minimum value is about 200 W/m^2, occurring around sunrise and sunset. This graph (Figure 2) shows the daily variation of temperature in the Bukhara region during the summer months of 2025. The temperatures, measured in Celsius, are plotted against time, labeled as “Time” on the axis. Starting from 7:12 in the morning, the temperature gradually rises from slightly above 30 ^{0}C and reaches over 40 ^{0}C in the afternoon, indicating the intense heat characteristic of the region. In the evening, a gradual decrease in temperature is observed.

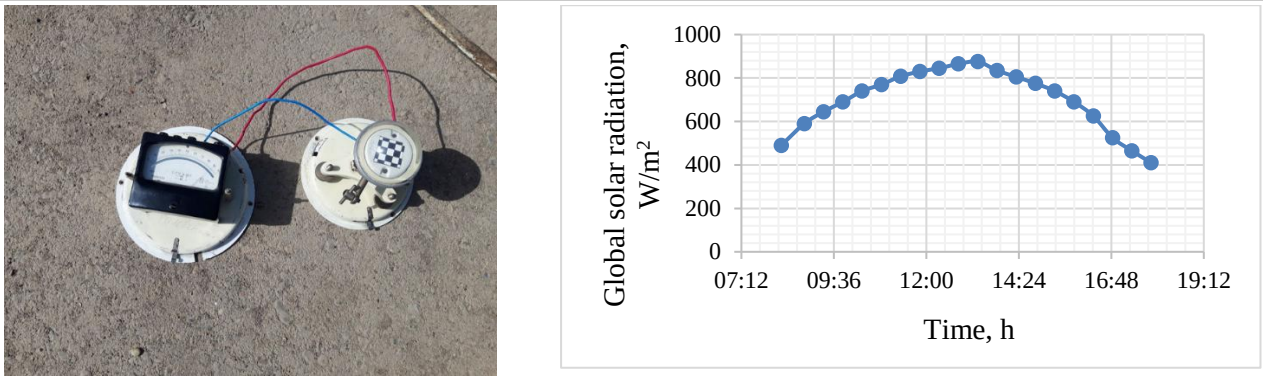

a) b)

Fig. 1. Pyranometer for measuring solar radiation (a) and daily solar radiation variation in studies (b).

These data illustrate the typical temperature variation of a hot day in Bukhara, which is important for understanding or planning around local climate changes, although the pattern becomes even clearer when compared with long-term historical temperature records. In some cases, temperature variations are also linked to wind direction and speed. In the analysis, the daily wind speed in the Bukhara region is plotted with time on the abscissa axis and wind speed on the ordinate axis (Figure 3), showing the average values of daily variation. The data reveal that the highest wind speeds reached around 4–5 m/s. Temperature gradients may be influenced by various factors such as geographical features and time of day.

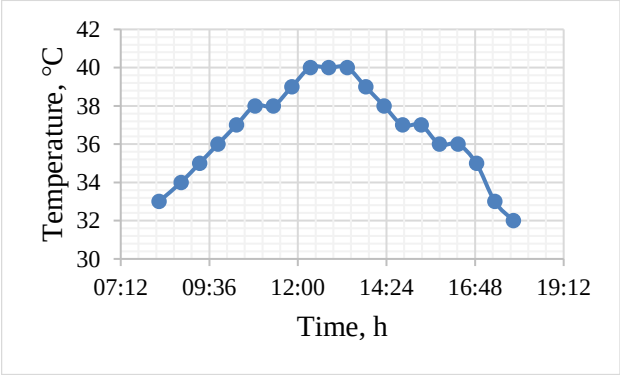

Fig. 2. Daily variation of ambient temperature

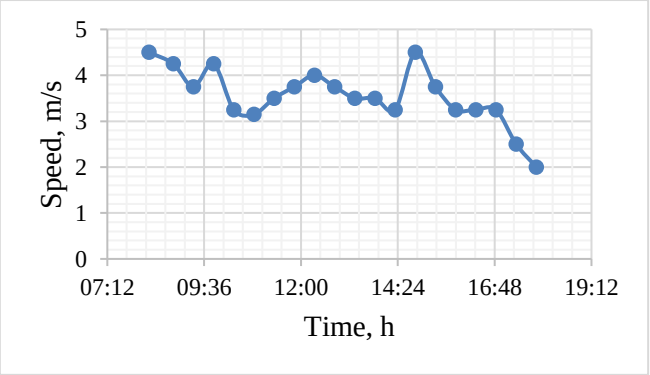

Fig. 3. Daily variation of wind speed

In our research, the daily dynamics of the inlet and outlet hot water temperatures in the experimental device were analyzed (Figure 4). The collector was connected to the reactor through pipes, through which hot water began to heat the water in the reactor tank. These values-the temperature of the water exiting the collector and heating the water in the reactor tank-were measured using a thermocouple. The average values of these measurements are presented in Figure 5.

The graph in Figure 5 illustrates the performance of the flat-plate solar collector, showing the dynamics of inlet (t_i) and outlet (t_o) temperatures at specific times of the day (from 7:12 to 19:12). The dashed line connected with red squares represents the outlet temperature, which rises rapidly in the morning, reaches close to 100 ^{0}C around midday, and then decreases again in the evening. In contrast, the inlet temperature of the heat-transfer fluid, shown with blue circles and a continuous line, remains stable and significantly lower, around 40 ^{0}C. During the daytime, the solar collector effectively absorbs solar energy, heating the heat-transfer fluid, which is then partially cooled when reintroduced into the biogas unit. Methane bacteria adapted to the operating temperature regime in bioreactors cannot function under sharply fluctuating temperatures [15-22]. From a physicochemical perspective, temperature stability is also critical for preventing degradation of thermally sensitive organic compounds and maintaining biochemical equilibrium. Experimental studies of thermally induced transformations in organic systems [23,24] confirm that even moderate temperature deviations may alter molecular stability and reaction kinetics. Therefore, maintaining controlled mesophilic conditions is not only a microbiological requirement but also a thermophysical constraint of the system.

Fig. 4. External appearance of the experimental setup

This graph shows the variation of biomass temperature in the bioreactor heated by a flat-plate solar collector throughout the day (from 7:12 to 19:12). The biomass temperature starts slightly above 30 ^{0}C, gradually rises to about 44 ^{0}C at midday, and then begins to decrease in the evening. These variation curves demonstrate the successful absorption of solar energy by the flat-plate solar collector and its transfer to the biomass. However, there is a need to stabilize this fluctuating temperature. To mitigate sharp changes, we used the daily loading dose intended for the bioreactor as a heating buffer [22]. This solar heating method highlights the direct correlation between the maximum accumulation of solar energy and the optimal temperature range for biomass, thereby increasing the likelihood of creating ideal conditions for metabolic processes [21,22]. During the day, solar radiation causes the temperature to rise, which enhances the metabolism responsible for biogas production. The differences between each measurement are relatively uniform, with no sharp increases or decreases, indicating stable conditions inside the bioreactor and a smooth process. The linear increase also suggests that, in the absence of additional feedstock, the substrate availability and microbial stability are maintained. Overall, the data reflect a healthy and stable biogas production process, dependent on the time of day, demonstrating both the efficiency of the solar collector and the influence of temperature on microbial activity within the bioreactor.

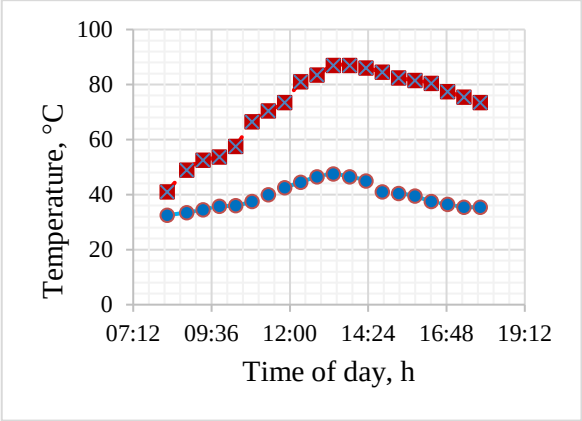

Fig. 5. Dynamics of inlet and outlet heat-carrying water temperature variation

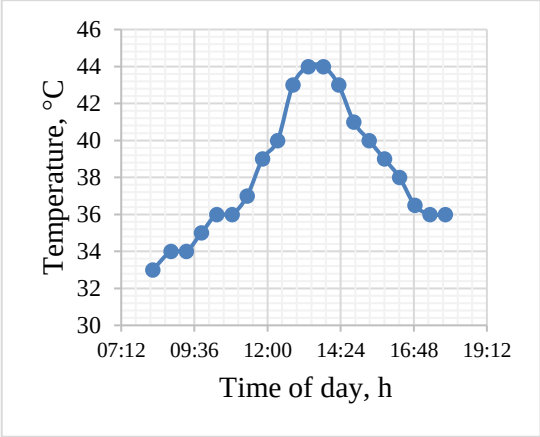

Fig. 6. Daily dynamics of temperature inside the bioreactor

In our research, the composition of biogas and the variation in methane content were analyzed. Biogas mainly consists of methane CH_4 and carbon dioxide (CO_2), along with about 2% trace gases (such as sulfur compounds, nitrogen oxides, S, NO). The primary economic indicator of this process is the methane content in the biogas, although in some cases, rapid processing of organic waste is also required.

Looking at the normalized data starting at 8:14, with subsequent times given in minutes, we observe a steady and gradual increase in biogas production. Biogas production starts at 0.1340 m^3 and continues until the end of the day, reaching 0.1570 m^3 from the baseline after 576 minutes (i.e., 9 hours and 36 minutes) from the

start time. The stable growth in biogas production is linked to various factors, such as the rise in temperature inside the bioreactor, since the bioreactor was heated using a solar collector [22].

3.2 Variation of biogas composition under mesophilic and psychrophilic temperature regimes

In practice, to increase the methane content of biogas, valuable methanogens are additionally loaded into bioreactors [15,16,25]. Introducing methanogens as simulators into small-capacity biogas units limits their use only to solving ecological problems [16-19]. In our research, the practical influencing factors on small-capacity biogas bioreactors are analyzed. Table 1: Standard and threshold indicators of biogas.

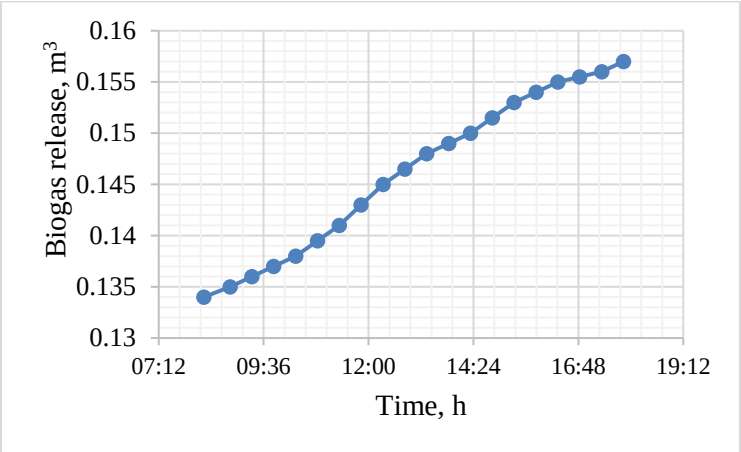

Fig. 7. Daily dynamics of temperature inside the bioreactor

In this context, the pH level is considered one of the main indicators of the anaerobic process occurring in small-capacity bioreactors. For biogas production, the required pH range is between 6.8 and 7.4. In many cases, when organic waste with high pH values (such as pigsty and poultry waste) is used, it is necessary to pass the units through a metabolic adaptation stage before operation [20-22]. The experimental study examines the composition of organic waste loaded into small-capacity units and their standard indicators (Table 1).

Table 1. Composition and standard indicators of the biomass loaded into the bioreactor.

Indicators	Standard values	Limit values
pH	6/8 – 7.4	6.4 – 7.8
Volatile fatty acids content (as CH_3COOH)	50 – 500 mg/l	200 mg/l
Total alkalinity (as $CaCO_3$)	500 – 1500 mg/l	1000 – 3000
Composition of produced gas	60 – 72% metan, 28 – 40% Carbon dioxide and other gases	
Salts		
NH_4 (as N)		300 mg/l.
Na		3500 – 5500 mg/l.
K		2500 – 4500 mg/l.
Ca		2500 – 4500 mg/l.
Temperature, °C	33 – 37	
Biogas production	0.3 – 0.52 m^3/kg based on dry organic matter	

The amount of volatile fatty acids should range from 50 to 500 mg/l. The threshold indicator is set at 200 mg/l [25]. In bioreactors, the total alkalinity of the organic waste load is required to be between 500 and 1500 mg/l. However, these specified conditions cannot be considered strict, since alkalinity in wastewater is highly variable, and levels ranging from 1000 to 3000 mg/l are also observed.

The salts most frequently and unsuccessfully involved in waste composition (NH_4, Na, K, and Ca) are required to remain within certain limits. The methane (CH_4) content in biogas obtained from different types of organic waste is shown in Table 2. As mentioned above, for anaerobic treatment of organic waste to produce

biogas, the ideal temperature should be around 38 ± 2^0C. It is necessary to select a regime suitable for the temperature to which methanogens have adapted. This table presents the types of organic waste, the amount of biogas obtained, and its composition. It is known that from cattle manure, 0.340 to 0.500 m^3 of biogas can be obtained per kilogram of dry matter (taking into account the duration of processing). The methane (CH_4) content of the resulting biogas is approximately 68%.

Table 2. Biogas yield and methane content from different types of organic waste

Animal manure	1 kg gas yield from dry matter, m^3	Methane storage, %
Cattle manure		
Pig manure	0.340 – 0.500	65.0
Poultry droppings	0.340 – 0.580	65 – 70
Fattening calf manure	0.310 – 0.620	60.0
Breeding calf manure	0.200 – 0.300	56 – 60
Organic waste from farms	0.300 – 0.620	70.0
Wastewater		
Vegetable residues	0.310 – 0.740	70
Potato residues	0.330 – 0.500	50 – 70
Beet residues	0.280 – 0.490	60 – 75
Plant waste	0.400 – 0.500	85
Straw		
Hay	0.200 – 0.300	50 – 60
Barley straw	0.200 – 0.300	59
Corn stalks	0.290 – 0.310	59
Flax	0.380 – 0.460	59
Beet pulp	0.360	59
Sunflower waste	0.165	59
Alfalfa	0.300	59
Other types	0.430 – 0.490	59
Green grasses		
Fallen leaves	0,280 – 0,630	70
Animal manure	0,210 – 0,290	58

Table 3 provides detailed information about the components of biogas and their properties: biogas composition and specific characteristics. The volumetric share of methane (CH_4) gas can range from 55 to 61% (in mixed organic waste), and from 62 to 72% (in single-type organic waste under warm climate conditions). The volumetric calorific value can reach 35.8 MJ/m^3 or higher. In our research, in order to increase the methane content, the biogas exiting the bioreactors was passed through a water filter (see Table 3).

Table 3. General specific characteristics of the average biogas obtained

Characteristics	Components of biogas				Biogas mixture ($60\%CH_4$+$40\%CO_2$)
	CH_4	CO_2	H_2	H_2S	
Volumetric fraction, %	55...70	27...44	<1	<3	10
Volumetric calorific value, MJ/m^3	35.8	–	10.8	22.8	21.5
Flammability limit (concentration in air), %	5...15	–	4...80	4...45	6...12
Ignition temperature, ^{0}C	650...750	–	585	–	650...750
Critical pressure, MPa	4.7	7.5	1.3	8.9	7.5...8.9
Critical temperature, ^{0}C	– 82.5	31.0	–	100	– 2.5
Normal density, g/l	0.72	1.93	0.09	1.54	1.2
Critical density, g/l	102	468	31	349	320
Density relative to air	0.55	2.5	0.7	1.2	0.83

3.3 Comparison with previous studies

The obtained experimental results were compared with published data on solar-assisted biogas systems and flat-plate solar collectors operating under mesophilic conditions [1-3, 15-25].

The measured solar collector efficiency (42–50%, average 42.6%) is consistent with values reported for conventional flat-plate collectors under high solar radiation levels (800 W/m^2), where efficiencies typically range from 35% to 55% depending on the heat-loss coefficient and operating temperature difference. The observed stagnation temperature behavior also agrees with analytical predictions reported in similar thermal studies. The biomass temperature in the reactor was maintained within 33 - 44 ^{0}C, corresponding to the mesophilic regime. Comparable systems described in the literature report temperature stabilization within 35-40 ^{0}C when external insulation and solar preheating are applied. The slightly wider temperature fluctuation observed in the present study is attributed to diurnal solar variability and wind-induced convective losses.

The annual biogas yield (932.535 m^3/year) and methane content (60-70%) are in agreement with reported values for cattle manure and mixed organic waste under mesophilic conditions, where specific yields typically range between 0.3 and 0.6 m^3/kg of dry organic matter. The methane fraction obtained after water filtration corresponds to published data on small-scale purification methods. Compared with previously reported small-capacity systems without enhanced insulation, the present configuration demonstrates reduced thermal losses and improved temperature stability, which directly contribute to sustained microbial activity and stable methane production.

4. Conclusion

Our research has shown that temperature plays a key role in maintaining the stability of the anaerobic fermentation process in small-scale biogas plants, and that the use of mathematical expressions for its calculation is important.

The results of studies conducted in rural conditions, using organic waste and small-scale biogas plants heated with solar energy, are presented. In the study, the design of the biogas plant was examined, including solar collectors, heat exchange elements, and thermal accumulators made of phase-change materials, which help maintain stable biomass temperature throughout the day.

During the experiments, solar radiation, ambient temperature, reactor temperature, and the daily dynamics of biogas production volume were analyzed. The results demonstrate that effective utilization of solar energy to ensure optimal temperature regimes in the bioreactor leads to stable growth in biogas production. The study also highlighted the influence of biomass type on the composition of the biogas produced. Temperature is the main factor for the stability of the anaerobic fermentation process, and its effective management emphasizes the importance of biomass processing efficiency.

Conflict of interest statement

The authors declare that they have no conflict of interest in relation to this research, whether financial, personal, authorship or otherwise, that could affect the research and its results presented in this paper.

CRediT author statement

Sharipov M.Z., Kovalev I.V. - Conceptualization, Methodology, Supervision; **Majitov J.A., Imomov Sh.J.:** Formal Analysis, Validation, Writing-Reviewing and Editing; **Narzullaev M.N., Negmatillayev B., Ziyoyev D.A. -** Investigation, Data curation, Writing - original draft. The final manuscript was read and approved by all authors.

References

1 Chen J. Heat-transfer Enhancement for Slurries from Biogas Plants- Properties, processes and thermal systems. *Diss…, Luleå: Luleå University of Technology*, 2022. https://www.researchgate.net/publication/389503732_Heat-transfer_Enhancement_for_Slurries_from_Biogas_Plants_-_Properties_processes_and_thermal_systems

2 Budhijanto W., Purnomo C.W. and Siregar N.C. (2012) Simplified Mathematical Model for Quantitative Analysis of Biogas Production Rate in a Continuous Digester. *Engineering Journal*, 16, 5, 167–176. https://doi.org/10.4186/ej.2012.16.5.167

3 Delgadillo Mirquez L., Machado Higuera M. and Hernández Sarabia M. (2018) Mathematical modelling and simulation for biogas production from organic waste. *International Journal of Engineering Systems Modelling and Simulation*, 10, 2, 97. https://doi.org/10.1504/IJESMS.2018.10013112.

4 Elsgaard L., Olsen A. B. and Petersen S. O. (2016) Temperature response of methane production in liquid manures and co-digestates. *Science of The Total Environment*, 539, 78–84. https://doi.org/10.1016/j.scitotenv.2015.07.145.

5 Bai Y., Yang M., Wang Z., Li X. and Chen L. (2019) Thermal stratification in a cylindrical tank due to heat losses while in standby mode. *Solar Energy*, 185, 222–234, https://doi.org/10.1016/j.solener.2018.12.063.

6 Ohk S.M. and Chung B.J. (2017) Natural convection heat transfer inside an open vertical pipe: Influences of length, diameter and Prandtl number. *International Journal of Thermal Sciences*, 115, 54–64, https://doi.org/10.1016/j.ijthermalsci.2017.01.014.

7 Perrigault T., Weatherford V., Martí-Herrero J. and Poggio D. (2012) Towards thermal design optimization of tubular digesters in cold climates: A heat transfer model. *Bioresour Technol*, 124, 259–268. https://doi.org/10.1016/j.biortech.2012.08.019.

8 Sharipov M., Majitov J., Ergashev S., Shodiyev E., Narzullayeva Z. (2025) Substitution Of Thermal-Technical and Geometric Parameters of A Small-Scale Biogas Plant. *Eurasian Physical Technical Journal*, 22(3-53), 84–90. https://doi.org/10.31489/2025N3/84-90

9 Sharipov L.A., Imomov S.J., Majitov J.A., Sharipov M.Z., Pulatova F., Abdisamatov O.S. (2020) Modeling of heat exchange processes in the Metanetka bioenergy plant for individual use. *Iop Conference Series Earth and Environmental Science*, 2020, 614(1), 012035. https://doi.org/10.1088/1755-1315/614/1/012035

10 Majitov J.A., Kamilov O.S., Yuliyev O.O. (2024) Solar biogas plant. Utility model patent No. FAP 2440. Published 19.03.2024. [in Uzbek] https://im.adliya.uz/document/check/e00d4d85-4e28-4988-917b-eb8f60e58fb7

11 Komilov O.S., Astanov S.Kh., Safarov O.F., Sharipov M.Z., Faizullaev A.R., Tillaev L. (2009) Combined solar drying unit. *Applied Solar Energy English Translation of Geliotekhnika*, 45(4), 262–265. https://doi.org/10.3103/S0003701X09040082

12 Mukhamadiev B.T., Sharipov M.Z. (2021) To the issue of organization of the communication system in microorganisms. *Iop Conference Series Earth and Environmental Science*, 848(1), 012224. https://doi.org/10.1088/1755-1315/848/1/012224

13 Mamatkarimov O, Ergashev O, Giyasidinov A, Sharipov M, Abrorov A, Khakimova N, Kovalev I. (2024) Overview of the IX International Conference on Advanced Agritechnologies, Environmental Engineering and Sustainable Development-AGRITECH-IX-2023, *E3S Web of Conferences.* 486, 00001. https://doi.org/10.1051/e3sconf/202448600001

14 Amon B. and C. A. Amon (2001) Emissions of NH_3, N_2O and CH_4 from dairy cows housed in a farmyard manure tying stall (housing, manure storage, manure spreading). Nutrient Cycling in Agroecosystems, 60(1):103-113. https://doi.org/10.1023/A:1012649028772

15 Talukdar D., Tsubokura M., (2022) Numerical study of natural-convection from horizontal cylinder at eccentric positions with change in aspect ratio of a cooled square enclosure. *Heat and Mass Transfer*, 58, 5, 849–871. https://doi.org/10.1007/s00231-021-03145-3.

16 Sebastian G., Shine S. R. (2015) Natural convection from horizontal heated cylinder with and without horizontal confinement. *Int J Heat Mass Transf*, 82, 325–334. https://doi.org/10.1016/j.ijheatmasstransfer.2014.11.063.

17 Fleming J.G. Novel simulation of anaerobic digestion using computational fluid dynamics. *North Carolina: North Carolina State University*, 2002. http://www.lib.ncsu.edu/resolver/1840.16/4158

18 Kalendar A., Alhendal Y., Hussain S., Karar S. and Oosthuizen P. (2021) Natural Convective Heat Transfer from Vertical Isothermal Polygonal Cylinders. *J. Thermophys Heat Trans*, 35, 4, 854–868, https://doi.org/10.2514/1.T6207.

19 Oosthuizen, P., Kalendar, A. (2014) Natural Convective Heat Transfer from Short Rectangular Cylinders Having Exposed Upper Surfaces and Mounted on Flat Adiabatic Bases. In: Natural Convective Heat Transfer from Short Inclined Cylinders. SpringerBriefs in Applied Sciences and Technology. Springer, Cham. https://doi.org/10.1007/978-3-319-02459-2_4

20 Kishor J., Goyal I. C., Sawhney R. L., Singh S. P., Sodha M. S. and Dayal M.(1988) Solar assisted biogas plants III: Energy balance of fixed dome biogas plants and enhancement of production in winters. *Int J Energy Res*, 12, 4, 711–737. https://doi.org/10.1002/er.4440120411.

21 Majitov J.A. (2020) Selection of design methodology for biogas facilities and assessment of economic efficiency. *Scientific and technical journal of the development of science and technology*, 7.129-134. [in Uzbek] https://journal.bmti.uz/?page_id=31

22 Majitov J.A. (2025) *Kichik quvvatli biogaz qurilmasining issiqlik-texnik parametrlarini asoslash. dis.PhD,* Qarshi. 71-74. https://library.ziyonet.uz/ru/book/135481

23 Astanov S., Sharipov M.Z., Faizullaev A.R., Kurtaliev E.N., Nizomov N. (2014) Thermal Destruction of Riboflavin in Different Aggregate States, *Journal of Applied Spectroscopy*, 81(1), 37-42. https://doi.org/10.1007/s10812-014-9883-z

24 Astanov S.K., Sharipov M.Z., Kasimova G.K. (2019) Hipochromic effect in riboflavin solutions, *Eurasian Physical Technical Journal*, 16(1), 12–17. https://doi.org/10.31489/2019no1/12-17

25 Rennie T. J., Baldé H., Gordon R. J., Smith W. N. and Vander Zaag A. C. (2017) A 3-D model to predict the temperature of liquid manure within storage tanks. *Biosyst Eng*, 163, 50–65. https://doi.org/10.1016/j.biosystemseng.2017.08.014.

AUTHORS' INFORMATION

Sharipov, Mirzo – Doctor of Physical and Mathematical Sciences, Professor, Head of Department of Physics, Bukhara State University, Bukhara, Uzbekistan; SCOPUS Author ID: 24177719300, https://orcid.org/0000-0003-0370-8066; m.z.sharipov@rambler.ru

Majitov, Jurabek – Doctor PhD, Associate professor, Physics Department Bukhara State Technical University, Bukhara, Uzbekistan; SCOPUS Author ID: 57221226030; https://orcid.org/0009-0005-9453-279X; majitov@mail.ru

Imomov, Shavkat – Doctor of Technical Sciences, Professor, National research university "Tashkent institute of irrigation and agricultural mechanization engineers" National research university, Tashkent, Uzbekistan; Scopus Author ID:57211805830, https://orcid.org/0009-0001-0191-7430; Researcher ID: T-3711-2018; Shavkat-imomov@rambler.ru

Kovalev, Igor - Doctor of Technical Sciences, Professor, Siberian Federal University, Krasnoyarsk, Russia; SCOPUS Author ID: 57360606900, https://orcid.org/0000-0003-2128-6661; kovalev.fsu@mail.ru

Narzullayev, Mukhiddin - Master, Senior Lecturer, Physics Department, Bukhara State Pedagogical Institute Bukhara; Uzbekistan; SCOPUS Author ID: 57221226030; https://orcid.org/0009-0000-5004-7315; muxiddin2024@mail.ru

Negmatillayev, Baxodir – Master, Senior Lecturer at the Department of Architecture, Bukhara State Technical University, Bukhara, Uzbekistan; https://orcid.org/0009-0000-9460-4478. bakhodir.negmatillayev@mail.ru

Ziyoyev, Dilshod – Master, Laboratory manager, Bukhara State Technical University, Bukhara, Uzbekistan; https://orcid.org/0009-0005-2202-6222; dilshodbek_ziyoyev@mail.ru